© 2014. Published by The Company of Biologists Ltd | Development (2014) 141, 3134-3142 doi:10.1242/dev.110395

RESEARCH ARTICLE

STEM CELLS AND REGENERATION

Deadenylase depletion protects inherited mRNAs in primordial germ cells

S. Zachary Swartz[1], Adrian M. Reich[1], Nathalie Oulhen[1], Tal Raz[2], Patrice M. Milos[2], Joseph P. Campanale[3], Amro Hamdoun[3] and Gary M. Wessel[1,*]

ABSTRACT

A crucial event in animal development is the specification of primordial germ cells (PGCs), which become the stem cells that create sperm and eggs. How PGCs are created provides a valuable paradigm for understanding stem cells in general. We find that the PGCs of the sea urchin *Strongylocentrotus purpuratus* exhibit broad transcriptional repression, yet enrichment for a set of inherited mRNAs. Enrichment of several germline determinants in the PGCs requires the RNA-binding protein Nanos to target the transcript that encodes CNOT6, a deadenylase, for degradation in the PGCs, thereby creating a stable environment for RNA. Misexpression of CNOT6 in the PGCs results in their failure to retain Seawi transcripts and Vasa protein. Conversely, broad knockdown of CNOT6 expands the domain of Seawi RNA as well as exogenous reporters. Thus, Nanos-dependent spatially restricted CNOT6 differential expression is used to selectively localize germline RNAs to the PGCs. Our findings support a 'time capsule' model of germline determination, whereby the PGCs are insulated from differentiation by retaining the molecular characteristics of the totipotent egg and early embryo.

KEY WORDS: Germ line, PGC, CNOT6, CCR4, Nanos, Pumilio, Transcriptomics, Sea urchin

INTRODUCTION

The germ line provides an immortal link between generations by transmitting heritable information from parent to progeny. Specification of the animal germ line typically occurs during embryogenesis, when primordial germ cells (PGCs) fated to become the gamete-producing stem cells of the adult are segregated from somatic lineages. PGCs in the numerous species studied share common molecular signatures, including the RNA helicase Vasa, the translational repressor Nanos and the Argonaute family member Piwi (Ewen-Campen et al., 2010). Surprisingly, despite this conservation of gene expression, the developmental routes that lead to it are remarkably diverse. Strategies for PGC segregation can be considered within a continuum of inherited and inductive mechanisms. An example of the inherited mode is that of *Drosophila melanogaster*, the PGCs of which are the first cells to form in the embryo. Their specification involves maternally supplied determinant mRNAs and proteins, collectively called germ plasm, which is actively transported and inherited by the presumptive PGCs. Conversely, PGCs in the mouse are specified by inductive signaling originating from the extraembryonic ectoderm. Most knowledge regarding these disparate mechanisms comes from studies in *Drosophila*, *Caenorhabditis elegans*, zebrafish and mice (Ewen-Campen et al., 2010; Pehrson and Cohen, 1986; Seydoux and Braun, 2006; Tanaka and Dan, 1990; Yajima and Wessel, 2011, 2012).

Comparatively little is known about PGCs outside these groups. Echinoderms, a large and diverse phylum, form part of the sister group to the chordates. The best-studied examples of this group are the sea urchins, including *Strongylocentrotus purpuratus*. In this species, four PGCs called small micromeres (sMics) are created by an asymmetric division at the fifth embryonic cleavage (Ewen-Campen et al., 2010; Juliano et al., 2006; Pehrson and Cohen, 1986; Seydoux and Braun, 2006; Tanaka and Dan, 1990; Yajima and Wessel, 2011, 2012) (Fig. 3C). After their formation, the sMics divide once during gastrulation to give eight descendants. These cells then assort into larval niches called the coelomic pouches, which are the major contributors to the juvenile sea urchin (Pehrson and Cohen, 1986; Tanaka and Dan, 1990). The early creation of the sMics is perhaps suggestive of inherited specification; however, sea urchins do not possess a classically defined germ plasm of aggregated germ line determinants. Instead, germline RNAs, including those of Vasa and Seawi (a Piwi family member), are maternally deposited, broadly distributed in early embryos and later refined to the sMics during gastrulation (Juliano et al., 2006; Seydoux and Braun, 2006).

To better understand the specification of the sMics, we used a transcriptomic approach to identify sMic-enriched mRNAs. We learned that the sMics are broadly transcriptionally repressed and identified transcripts, like Vasa and Seawi, that are ubiquitous in the early embryo but are later turned over in somatic cells to result in sMic enrichment. The expression dynamics of these discovered transcripts imply a post-transcriptional mechanism by which sMics retain RNA. Transcriptome analysis identified the mRNA encoding the CCR4-related deadenylase CNOT6 as uniquely depleted in the sMics. This depletion is dependent upon the RNA-binding protein Nanos and sequence elements in the CNOT6 3′ UTR that match the highly conserved binding consensus for Pumilio, the binding partner of Nanos. Depletion of CNOT6 is required for retention of Vasa protein and Seawi RNA in the sMics.

RESULTS

Differential expression analysis and identification of sMic-enriched transcripts

We developed a method for isolating PGCs *en masse*. In *S. purpuratus*, the sMics selectively retain the fluorescent dye calcein due to altered multidrug transporter activity (Campanale and Hamdoun, 2012) (Fig. 1A,B), even when dissociated into single-cell suspensions (Fig. 1C). We purified sMics by fluorescence-activated cell sorting (FACS), which yielded approximately 0.5%

[1]Department of Molecular, Cellular Biology and Biochemistry, Brown University, Providence, RI 02912, USA. [2]Helicos BioSciences Corporation, One Kendall Square, Building 700, Cambridge, MA 02139, USA. [3]Marine Biology Research Division, Scripps Institution of Oceanography, University of California at San Diego, 8750 Biological Grade Road, La Jolla, CA 92037, USA.

*Author for correspondence (rhet@brown.edu)

Received 20 March 2014; Accepted 22 June 2014

Development (2014) 141, 3134-3142 doi:10.1242/dev.110395

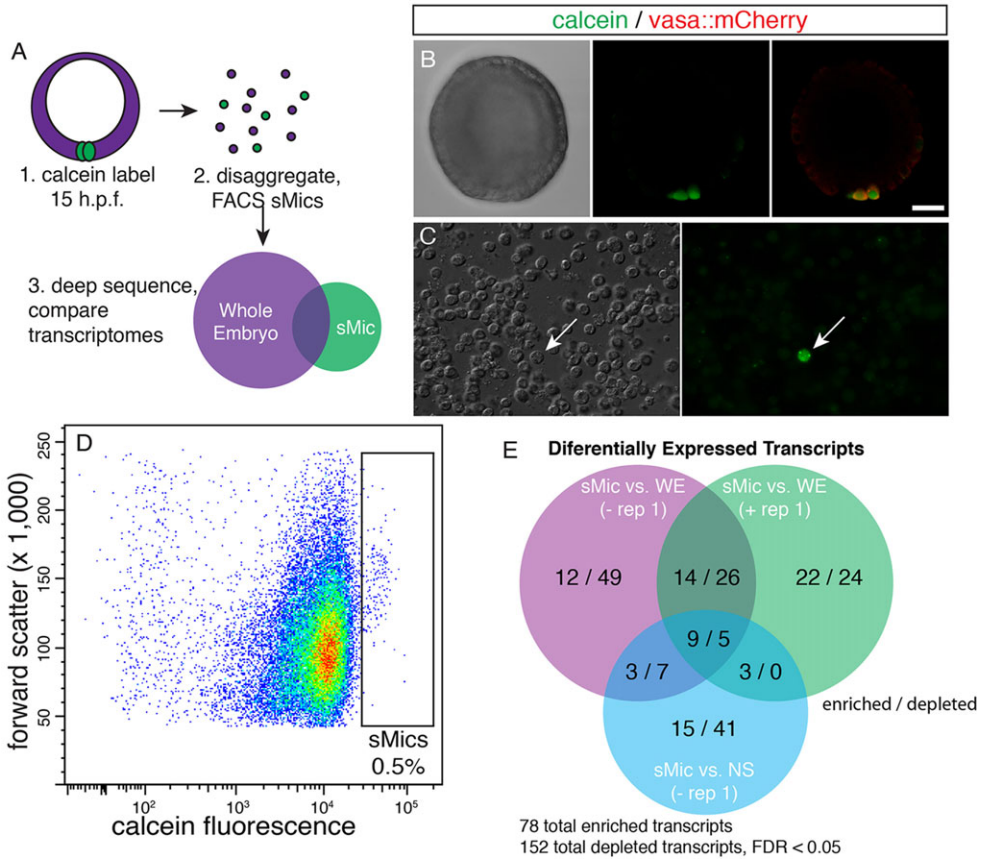

Fig. 1. FACS isolation and deep sequencing of sMics. (A) Schematic diagram depicting FACS isolation, RNA deep sequencing and differential expression analysis. (B) sMics accumulate the fluorescent dye calcein at 15 hpf. sMics are co-labeled with an mCherry fusion reporter of Vasa, a conserved germline RNA helicase that localizes post-translationally. (C) Calcein labeling is retained in blastomeres dissociated at 15 hpf. Arrows indicate labeled sMic. (D) Representative scatter plot of sMics collected by FACS, plotted as forward scatter versus calcein fluorescence. Cells collected as putative sMics are indicated by the box, which represents 0.5% of the total cell sample. (E) Venn diagram summarizing the number of sMic-enriched and -depleted transcripts discovered in three differential expression comparisons with FDR<0.05: sMic versus whole embryo (WE) and sMic versus non-sMics (NS), with and without replicate 1 included. Transcript totals are given as sMic-enriched/sMic-depleted. Scale bar: 20 µm.

of the total population of the embryo (Fig. 1D; supplementary material Fig. S1A-F). By qPCR, isolated calcein-positive cells were 16-fold enriched for Nanos, a known sMic-specific transcript, but were not enriched for Spec, an ectodermal transcript (supplementary material Fig. S1G). With this indication of purity, total RNA was then isolated and deep-sequenced without amplification from three biological replicates: isolated sMics, non-sMics and disaggregated whole embryos. After assessing variation between samples by multidimensional scaling (MDS) analysis, we performed differential expression analysis to discover sMic-enriched and -depleted transcripts (supplementary material Fig. S1H-J). In summary, with a significance cutoff of 0.05 (false discovery rate, FDR), we identified a union set of 230 differentially expressed transcripts (both sMic enriched and depleted) between these comparisons (Fig. 1E; supplementary material Fig. S1I,J; Tables S7-S9).

The sMic-enriched transcripts included Nanos and Delta, which have previously been identified as sMic-localized, as well as SpG-cadherin, which is required for sMic fate in *S. purpuratus* and is enriched in the sMics of *Lytechinus variegatus* (Juliano et al., 2010; Miller and McClay, 1997; Oliveri et al., 2002; Yajima and Wessel, 2012). The sMic-enriched transcripts fell into diverse functional categories, but transcriptional regulation and RNA binding were overrepresented according to a gene set enrichment analysis (supplementary material Table S1). Several sMic transcripts lie within the same pathway. For example, we identified the DNA-binding factor Baf250 and the ATPase Brg1, which both assemble into the pluripotency-associated esBAF chromatin remodeling complex (Lessard and Crabtree, 2010). In addition to Delta, we also identified MibL, a potential regulator of Notch/Delta signaling (Le Borgne and Schweisguth, 2003).

The sMics are broadly transcriptionally repressed

Surprisingly, the majority of sMic-enriched transcripts we discovered appear to be maternally deposited. To examine temporal expression dynamics of sMic-enriched genes, we used a microarray dataset containing the whole-embryo expression level of all genes at multiple time points (Wei et al., 2006). On average, sMic transcripts were at maximum abundance at 2 and 15 hours post fertilization (hpf) (Fig. 2A). sMic transcripts then sharply dropped in abundance at 30 hpf, just after the onset of gastrulation. By calculating the 30 h/15 h abundance ratio, we found that sMic transcripts were statistically overrepresented for decreasing abundance compared with the whole-transcriptome average and with sMic-depleted transcripts (Fig. 2B). These dynamics suggest maternal loading followed by broad turnover. sMic nuclei are depleted for RNA polymerase II phosphorylated at serine 2 of the C-terminal domain, a marker of transcriptional elongation (Fig. 2C,D) (Seydoux and Dunn, 1997). This depletion is first apparent at blastula stage and persists through gastrulation. Furthermore, sMic nuclei are highly enriched for histone 3 lysine 9 trimethylation (H3K9me3), a heterochromatin marker (Fig. 2E,F). Thus, we infer that sMics are transcriptionally repressed relative to their somatic neighbors. Furthermore, we did not detect transcripts that accumulated exclusively in the sMics. In this regard, Nanos remains the unique exception (Fig. 3A). Rather, sMic transcripts were broadly detectable in eggs and early embryos until blastula-to-gastrula stage, when broad turnover occurs in all cells except the sMics. Such genes include *Baf250*, *Ctdspl2*/*SCP2* [an RNA polymerase II (RNAPII) C-terminal domain phosphatase], *z62* (a C2H2 zinc-finger protein) and *MibL* (Fig. 3B; supplementary material Fig. S2A-F). These observations suggest that sMics retain maternally loaded and zygotically transcribed transcripts, which are cleared from somatic cells during the blastula-to-gastrula transition. Given this repression

Development (2014) 141, 3134-3142 doi:10.1242/dev.110395

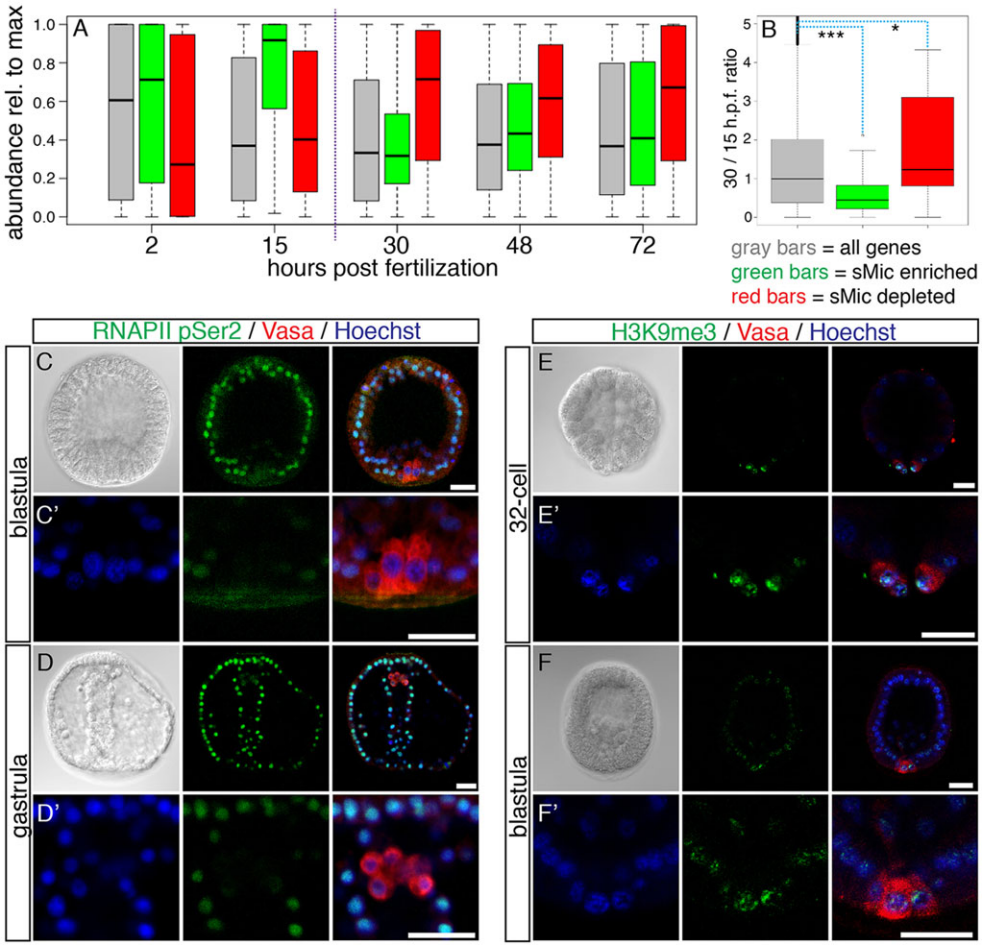

Fig. 2. Transcriptional repression in sMics. (A) Box and whisker plots summarizing average relative abundance of sMic-enriched (green bars), sMic-depleted (red bars) and all transcripts (gray bars) in the microarray study at five developmental time points between 2 and 72 hpf. On average, sMic-enriched transcripts reach their maximum abundance before 30 hpf and then decrease. Conversely, sMic-depleted transcripts reach their maximum after 30 hpf. An average of all genes in the microarray study remains relatively constant through development. (B) Ratio of average expression levels from 15 to 30 hpf for sMic-enriched (green bars), sMic-depleted (red bars) and all transcripts (gray bars). ***P=1.076e-06, *P=0.001357 (Mann–Whitney U-test). (C-D′) Immunofluorescence signal for RNAPII pSer2 (green) is depleted in sMics of blastula (C,C′) and gastrulae (D,D′). (E-F′) H3K9me3 (green) immunofluorescence is enriched in sMics in 32-cell embryos (E,E′) and blastulae (F,F′). (C′,D′,E′,F′) Higher magnification views of the sMics, labeled with Vasa antibody (red) (Voronina et al., 2008). Scale bars: 20 µm.

and the sMic transcript dynamics, we suggest that sMics inherit and retain their select mRNAs rather than actively transcribing them (with the important exception of Nanos).

CNOT6 transcript is selectively degraded in the sMics by a Nanos/Pumilio-dependent mechanism

Our transcriptome analysis and *in situ* hybridizations imply a mechanism by which the sMics stably retain inherited RNA. In addition, we previously found that RNA microinjected into the fertilized egg is degraded in resultant somatic cells but retained in sMics, independently of its sequence (Gustafson and Wessel, 2010; Oulhen and Wessel, 2013). Our study offers an explanation for these phenomena: the top sMic-depleted transcript encodes CNOT6 (FDR=2.40E-13), an ortholog of CCR4 and a broadly conserved deadenylase subunit of the conserved CCR4/POP2/NOT complex (Collart and Panasenko, 2012). As a major regulator of RNA stability, depletion of CNOT6 could enhance RNA retention. By fluorescence *in situ* hybridization (FISH), CNOT6 transcript is detectable ubiquitously in eggs through 32/60-cell embryos (Fig. 3D-F), but the transcript is uniquely depleted in the sMics by blastula stage (Fig. 3G-I). Nanos is a strong candidate for mediating this depletion. In diverse species, Nanos and its binding partner Pumilio recognize highly conserved motifs in the 3′ UTRs of target transcripts, termed Pumilio response elements (PREs), leading to mRNA degradation (Chen et al., 2012; Gerber et al., 2006; White et al., 2001; Wreden et al., 1997). The three *S. purpuratus* Nanos paralogs are each expressed in the sMics and are required for their survival (Juliano et al., 2010). Furthermore, we find that the 3′ UTR of CNOT6 contains two PRE sequences, suggesting that it is a Nanos/Pumilio target (supplementary material Fig. S3). We therefore knocked down Nanos with a translation-blocking morpholino antisense oligo (MASO) targeting the two most abundant of the three paralogs. This previously characterized MASO results in the eventual death of the sMics, and its effects were rescued by expression of a MASO-insensitive Nanos construct, thereby demonstrating specificity (Juliano et al., 2010). In morphant embryos, CNOT6 mRNA accumulated in sMics (Fig. 4A,B). We next tested the two putative PREs as sequence-specific targets with MASOs complementary to these two sites, which we predicted would occlude binding of Nanos/Pumilio. Consistent with Nanos knockdown, PRE-protecting MASOs caused retention of CNOT6 mRNA in the sMics (Fig. 4C). To further test the motifs, we used reporter constructs containing either the full-length wild-type CNOT6 3′ UTR, or the full-length UTR with the PREs mutated singly or in combination (Fig. 4D-H). The wild-type reporter recapitulated the sMic exclusion of the endogenous transcript (Fig. 4E); however, mutations of the PREs resulted in sMic retention (Fig. 4F-H). In further support of its role, Pumilio co-immunoprecipitates with Nanos (supplementary material Fig. S4A). We attempted to test the effect of Pumilio knockdown on CNOT6 accumulation; however, these embryos were developmentally arrested before blastula stage, probably pointing to pleiotropic effects (data not shown). Indeed, Nanos-independent roles for Pumilio have been identified (Van Etten et al., 2012; Weidmann and Goldstrohm, 2012). Indicative of its diverse functions, Pumilio protein is detectable in granules in all cells of the

Development (2014) 141, 3134-3142 doi:10.1242/dev.110395

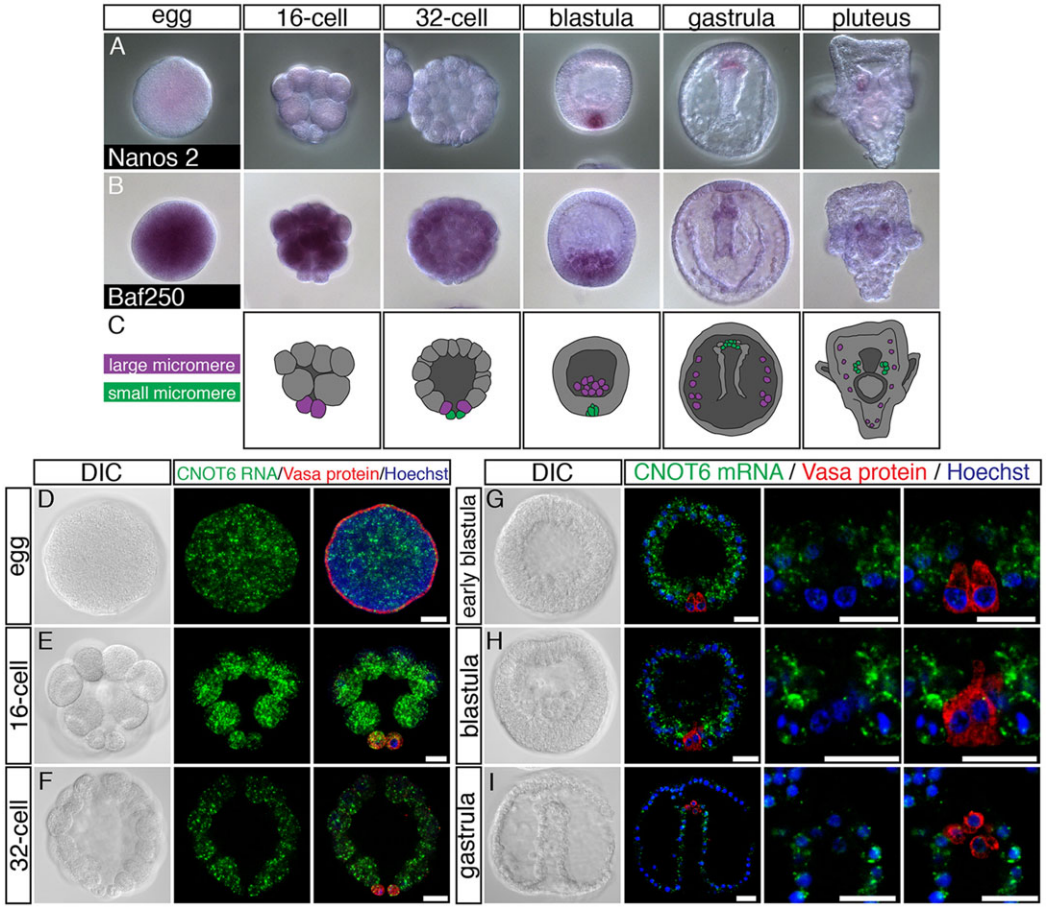

Fig. 3. Localization of differentially expressed transcripts. (A,B) *In situ* hybridizations for sMic-enriched transcripts Nanos2 and Baf250. In contrast to Nanos, Baf250 transcript is detectable in eggs and is broadly distributed until blastula stage, when its localization is refined to the sMics. (C) Schematic depiction of the micromere lineage in early development. (D-I) FISH for CNOT6 transcript (green). CNOT6 transcript is depleted in the sMics (labeled by Vasa antibody, red) by blastula stage and remains depleted through gastrulation, after which it becomes undetectable. Scale bars: 20 µm.

early blastula and is highly enriched in the Veg2 mesodermal precursors of later blastulae (supplementary material Fig. S4C,D). Nanos-mediated degradation of CNOT6 transcript is surprising, especially in light of evidence that Nanos functions by recruiting the CCR4-NOT complex itself (Suzuki et al., 2012). One possibility is that the CCR4-NOT complex maintains functionality with only the Pop2-related nuclease CNOT7, which is present in sMics at the transcript level (supplementary material Fig. S2G). Alternatively, maternal CNOT6 protein may be initially available in the sMics to degrade the mRNA, but then turned over later. Both possibilities are consistent with our conclusion that Nanos/Pumilio directs degradation of maternal CNOT6 mRNA in the sMics via PRE motifs in its 3′ UTR.

CNOT6 repression is required for retention of germline determinants

To test the requirement of CNOT6 repression for germline fate, we misexpressed CNOT6 in the sMics by multiple approaches. A CNOT6::mCherry fusion construct that expresses in all cells significantly reduced accumulation of a previously characterized sMic reporter, Vasa::GFP (Fig. 5A-C) (Gustafson et al., 2011). We next tested the accumulation of endogenous Vasa protein. Embryos were fixed at 42 hpf, following gastrulation and one division of the sMics, resulting in approximately eight descendants on average. Both CNOT6::mCherry, as well as PRE-protecting MASOs, predicted to stabilize endogenous CNOT6 in the sMics, resulted in significantly fewer Vasa protein-positive sMics (Fig. 5D-G). This observation could be explained by a failure in mitosis, cell death or loss of Vasa protein in the sMics. To distinguish between these possibilities, we stably labeled the sMic lineage by 5-ethynyl-2′-deoxyuridine (EdU) incorporation. Due to their slow cell cycle, sMics retain EdU pulsed before first cleavage, compared with other more rapidly dividing cells, enabling definitive lineage analysis (Tanaka and Dan, 1990). Both control and CNOT6-overexpressing embryos possessed similar numbers of sMics, indicating a loss of inherited determinants, but no other defects (Fig. 6D). Endogenous Vasa is probably lost later than the reporter construct (Fig. 5A-C) because of the abundance of maternally supplied Vasa protein, whereas injection of reporter RNA requires new translation (Voronina et al., 2008). Additionally, we tested the transcript abundance of the endogenous Argonaute family member Seawi in the sMics with CNOT6 overexpression. Seawi transcript is normally present in all cells but is highly enriched in the sMics (Yajima et al., 2013). With CNOT6::mCherry expression, the sMics lose enrichment for Seawi RNA (Fig. 6A-C). We conclude that CNOT6 depletion is necessary for retention of germline determinants in the sMics.

Repression of the CNOT6 deadenylase may allow for increased background stability for inherited RNAs in the sMics. Therefore, we predicted that global CNOT6 knockdown would expand the domain of RNA retention. CNOT6 is required for normal development of the embryo; strong knockdown leads to profound endomesodermal defects (supplementary material Fig. S4E,F). We therefore tested

Development (2014) 141, 3134-3142 doi:10.1242/dev.110395

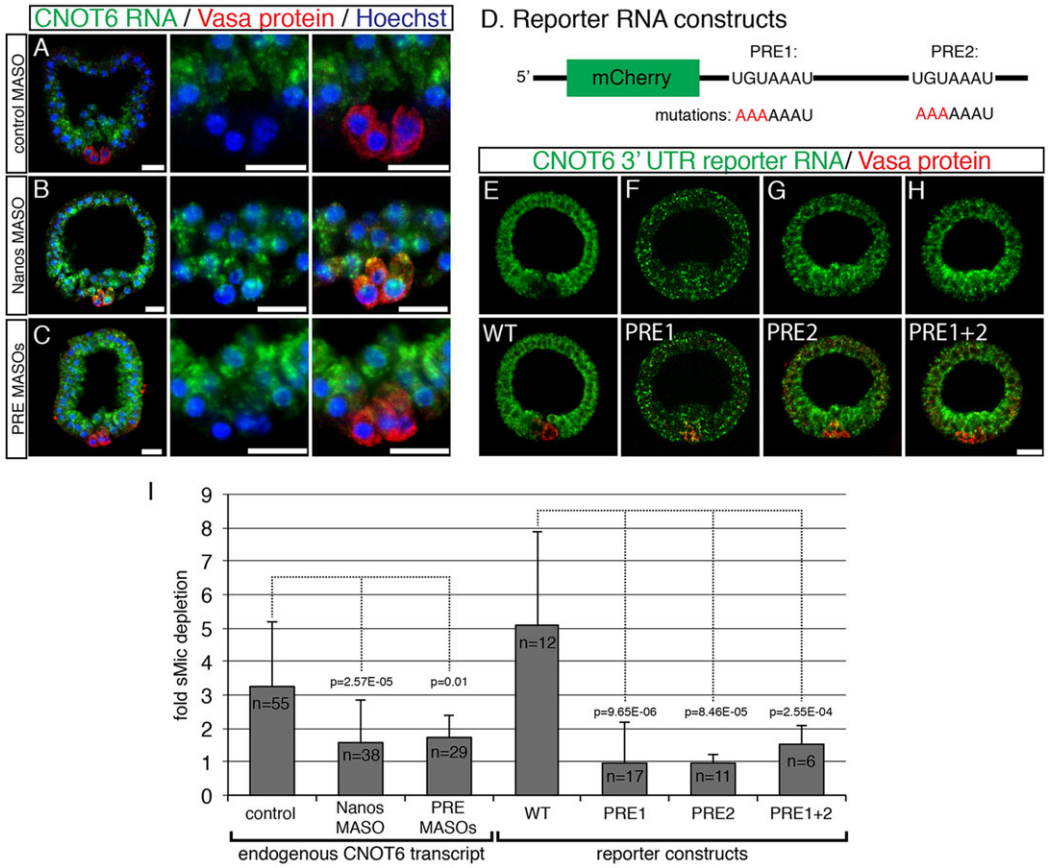

Fig. 4. CNOT6 mRNA depletion **in the sMics requires Nanos.** (A,B) MASO knockdown of Nanos de-represses CNOT6 transcript in the sMics compared with control embryos. (C) Co-injection of MASOs targeting the two PREs also de-represses CNOT6 transcript in sMics. (D-H) A synthetic reporter construct (D) containing the full-length CNOT6 3′ UTR recapitulates the localization of endogenous CNOT6 transcript (E). Mutating putative PRE sequences alone (F,G) or in combination (H) de-represses reporter accumulation in the sMics. (I) Pixel intensity quantitation of fold depletion in sMics versus the rest of the embryo for endogenous CNOT6 and reporter transcripts. *P*-values are calculated by two-tailed unpaired *t*-test. Scale bars: 20 µm.

the effects of weaker CNOT6 knockdown (under which development proceeds relatively normally) on Seawi transcript localization. In control embryos, Seawi transcripts are highly enriched in the sMics. However, when we globally reduce CNOT6 protein with either of two non-overlapping MASOs, Seawi transcripts are more broadly retained throughout the endomesoderm and oral ectoderm (Fig. 6E-H). To test the generality of CNOT6-mediated RNA retention, we used exogenous RNA encoding mCherry with an SV40 3′ polyadenylation signal. As reported for other exogenous RNAs, this transcript is retained in the sMics but is degraded in somatic cells in a sequence-independent manner (Fig. 7A) (Gustafson and Wessel, 2010; Oulhen and Wessel, 2013). However, when CNOT6 is globally depleted, mCherry RNA is retained throughout the endomesoderm (Fig. 7B,C). Our results indicate that differential CNOT6 expression is crucial for proper accumulation of transcripts within the sMics and is required for normal development of somatic lineages.

DISCUSSION

Our study reveals mechanistic insight into the divergence of germ line from soma. Uniformly dispersed mRNAs in the early embryo become highly asymmetric by the selective Nanos/Pumilio-mediated repression of CNOT6 in the germ cell precursors. This paradigm explains the localization of known sMic-enriched mRNAs, including Vasa and Seawi (Juliano et al., 2006), as well as foreign transcripts introduced in the early embryo (Gustafson and Wessel, 2010; Oulhen and Wessel, 2013). The RNA retention mechanism via CNOT6 depletion raises the question: is there specificity in the RNAs that sMics retain or is the retention completely nonselective? Although our dataset is probably incomplete, if retention were completely nonselective, one would expect to identify more than the 78 sMic-enriched transcripts we report. It is possible that the sMics possess mechanisms to exclude RNAs – Nanos/Pumilio is one such example, although there might be others that remain uncharacterized. Indeed, through bioinformatics we identified numerous transcripts that are depleted in the sMics, and it will be important in the future to investigate the mechanisms of their depletion. The fact that sMics generally retain RNA is probably necessary because they are transcriptionally quiescent. Transcriptional repression has also been documented in *Drosophila*, *C. elegans*, ascidians and mice, indicating that it is a fundamental feature of germline segregation (Nakamura and Seydoux, 2008; Shirae-Kurabayashi et al., 2011). Surprisingly, however, each organism achieves repression via distinct mechanisms. Although the precise nature of sMic repression is unknown, we find that the RNAPII phosphatase Ctdspl2 is sMic-enriched, indicating one possible mechanism.

Broad clearance of maternal RNA is a hallmark of the maternal to zygotic transition (MZT), a conserved event when developmental control is passed to the embryo. In *Drosophila*, there are two phases of degradation: the first occurs following egg activation and involves the RNA-binding protein Smaug, which recruits the CCR4-NOT complex to degrade diverse targets (Semotok et al., 2005). The PGCs possess degradation activity, but certain transcripts are protected in

Development (2014) 141, 3134-3142 doi:10.1242/dev.110395

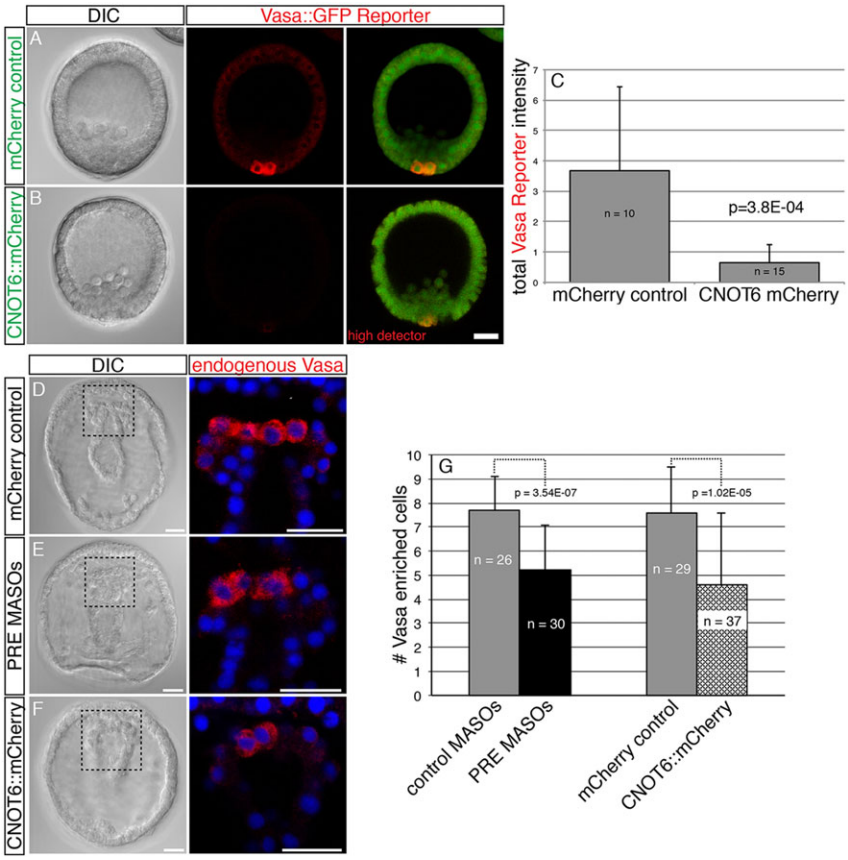

Fig. 5. CNOT6 depletion is required for sMic Vasa protein expression. (A,B) Expression of CNOT6::mCherry (green) in all cells significantly reduces Vasa::GFP reporter signal (red) compared with mCherry alone (control) in 20 hpf embryos. Images at higher detector settings are provided (right hand), indicating that the sMics are still present and weakly positive for Vasa::GFP. (C) Integrated pixel intensity data for mCherry control and CNOT6::mCherry misexpression embryos. (D,E) PRE-protecting MASOs result in significantly fewer Vasa-positive cells at 42 hpf. (F) Expression of CNOT6::mCherry in all cells, including the sMics, similarly reduces the number of Vasa-positive cells compared with expression of mCherry alone. (G) Counts of Vasa-enriched cells in control, PRE-protecting MASO and CNOT6 misexpression embryos. *P*-values are calculated by two-way unpaired *t*-test. Scale bar: 20 µm.

the PGCs by motifs in their 3′ UTRs, perhaps by Oskar association (Bashirullah et al., 1999; Zaessinger et al., 2006). A second degradation process is driven by the mir-309 cluster at about 2 hpf (Bushati et al., 2008). The piRNA pathway also contributes to degradation of Nanos transcript in somatic cells and involves the CCR4-NOT complex (Rouget et al., 2010). In zebrafish, a primary effector of maternal RNA degradation at the MZT is mir-430 (Giraldez et al., 2006). It has been further observed that some mir-430 targets, such as Nanos, are degraded in the soma but protected in the PGCs (Mishima et al., 2006). In the sea urchin, the zygotic genome activates shortly after fertilization. However, the degradation aspect of the MZT in the future soma might be conserved via CNOT6 and could include small RNA mechanisms (Song et al., 2012).

Prior to this study, the only known mechanisms for stabilizing RNA in the germ line were via Dead end 1 (Dnd1) and Deleted in azoospermia-like (Dazl), which work by occluding microRNA-binding sites and by promoting deadenylation, respectively (Kedde et al., 2007; Mishima et al., 2006; Takeda et al., 2009). However, Dnd1 is not conserved outside of vertebrates. We show here in an early branching deuterostome that the deeply conserved deadenylase CNOT6 is repressed in its PGCs by Nanos/Pumilio, allowing for stable retention of inherited transcripts. As the PGCs are transcriptionally repressed, their inheritance might represent a ‘time capsule’ of early development; that is, they must subsist solely on the mRNAs they retain from the egg, independently of a germ plasm (supplementary material Fig. S5). A consequence of this strategy might be that the PGCs remain insulated from differentiation into somatic lineages. Furthermore, our model is consistent with an immortal cytoplasm hypothesis for the evolutionary origin of the segregated germ line at the transition from unicellular to multicellular animal life. The ancestral single-celled organism probably possessed the highly conserved factors found in animal germ lines, which were retained at the transition to multicellularity (Extavour and Akam, 2003). It is the somatic cells that acquired unique characters to diversify from the original, progenitor cell type, while sacrificing reproductive potential (Buss, 1987; Extavour, 2007). The diversification of the soma may have necessitated the evolution of global turnover events (e.g. the MZT) to eliminate RNAs associated with the egg. Instead of acquiring gametogenic capability anew, the embryonic germ cells remain protected and retain the characteristics of the egg. Downregulation of deadenylase activity provides a mechanism for understanding how cytoplasm that confers gametogenic potential is preserved in the segregated germ line.

MATERIALS AND METHODS

Animals

S. purpuratus were maintained in aquaria containing artificial seawater at 16°C. Individuals were induced to shed gametes by shaking or by injection of 0.5 M KCl. Eggs were collected in filtered seawater (FSW) and sperm was collected dry. Eggs were fertilized in the presence of 1 mM 3-amino-triazol (3-AT) (Sigma) to prevent crosslinking of fertilization envelopes. Embryos were reared at 15°C at a density of about 0.2% (packed egg volume/seawater volume) in stirring culture vessels.

FACS isolation of sMics

Embryos were collected 15 hpf by straining through 45 µm Nitex and concentrated to about 0.5% density in 50 ml FSW. PSC833 (Novartis) and calcein AM (C-AM, Invitrogen) were added to the FSW at 500 nM and 250 nM, respectively. The embryos were then incubated for 90 min at 15°C with constant rotation in 50 ml conical tubes. Embryos were pelleted by centrifuging at 250 ***g*** for 30 s, washed twice in 50 ml of calcium-free seawater and then resuspended in a 10 ml 1 M glycine 25 mM EDTA solution. After incubating for 5 min on ice, the embryos were disaggregated by trituration through a transfer pipette 20 times. The single-cell suspension was pelleted

Development (2014) 141, 3134-3142 doi:10.1242/dev.110395

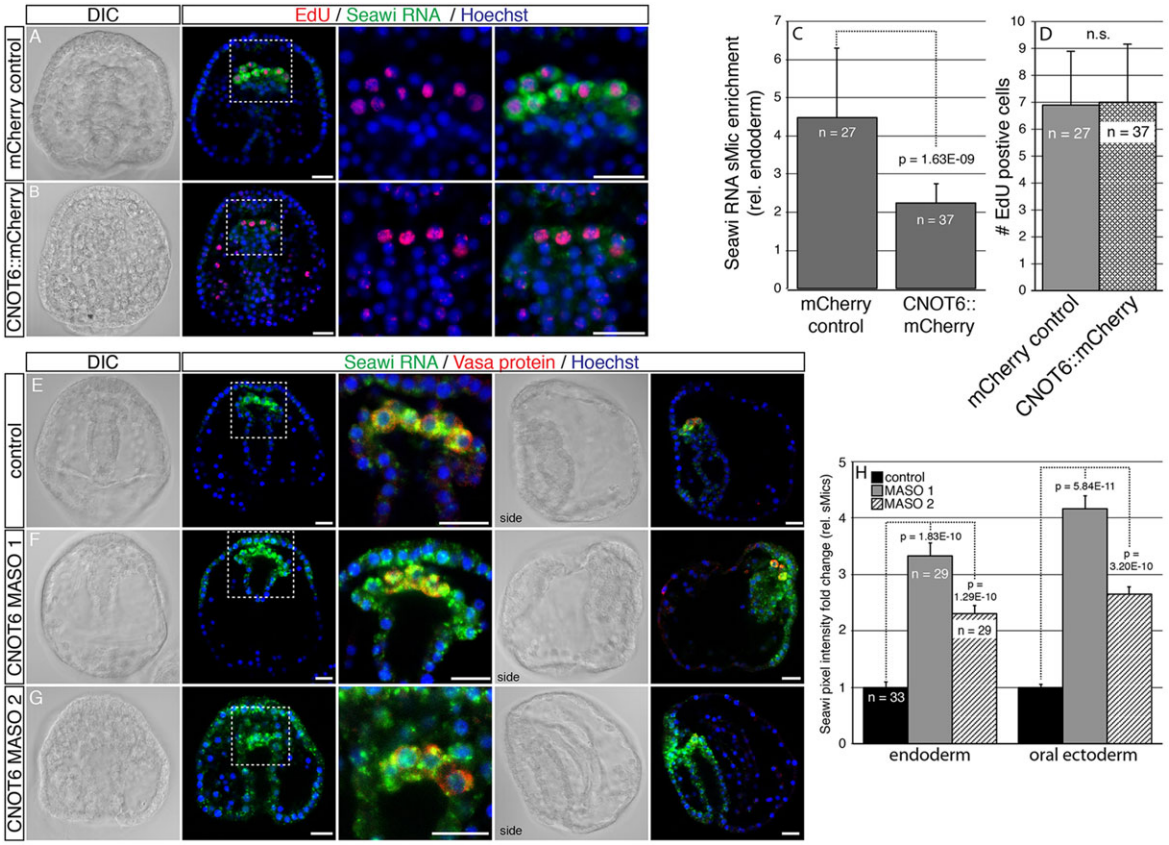

Fig. 6. CNOT6 mediates selective enrichment of Seawi transcript in the sMics. (A,B) Expression of CNOT6::mCherry in all cells reduces the enrichment of Seawi transcript in the sMics, detected by FISH (green), compared with mCherry alone controls. sMic lineage is traced by EdU incorporation (red). (C) Pixel intensity quantitation of Seawi transcript enrichment in sMics relative to the endoderm. (D) Counts of EdU-positive cells in mCherry control and CNOT6::mCherry-expressing embryos indicate no change in sMic numbers. sMics were counted by focusing through the gut tip; one representative focal plane is shown in B. (E-G) CNOT6 knockdown with either of two non-overlapping MASOs expands the domain of Seawi RNA into the endoderm and oral ectoderm at 42 hpf. (H) Fold change of Seawi FISH average pixel intensity in control and knockdown embryos, relative to sMic Seawi intensity. *P*-values are calculated by unpaired two-tailed *t*-test. Scale bars: 20 µm.

by centrifugation at 250 ***g*** for 5 min at 4°C, washed three times in calcium-free seawater to a final sample volume of 4 ml. PSC833 was then added to 1 µM final concentration. The cell suspension was sorted on a FACSAria instrument (BD Biosciences) set to 4°C. For long sorts, staggered cultures were fertilized at 2 h intervals, and then labeled and disaggregated at 15 hpf to avoid cell death and changes to their transcriptional profile. Cells were first gated by forward and side scatter to remove debris and aggregates, and then sorted by fluorescence intensity versus forward scatter. Cells were sorted directly into 0.75 ml Trizol LS (Invitrogen) until the total volume reached 1 ml. Sorts, numbers of collected cells and RNA extraction yields are summarized in supplementary material Table S2.

Helicos sample preparation and deep sequencing

RNA was extracted using Trizol LS reagent as described by the manufacturer (Invitrogen). RNA was treated using RQ1 DNAse (Promega) for 30 min at 37°C, then extracted with acid phenol:chloroform (Ambion). Three biological replicates of paired sMic, non-sMic and whole-embryo RNA were collected. Two replicate pairs were pooled from three separate sorts, whereas the third was collected from a single sort. Total RNA was stored in 100% ethanol, processed for RNA-seq without amplification or poly-A selection and sequenced by Helicos tSMS (Lipson et al., 2009). These quantitative short Helicos reads (averaging 30-35 nucleotides) were then mapped and counted to a *de novo* reference transcriptome generated using

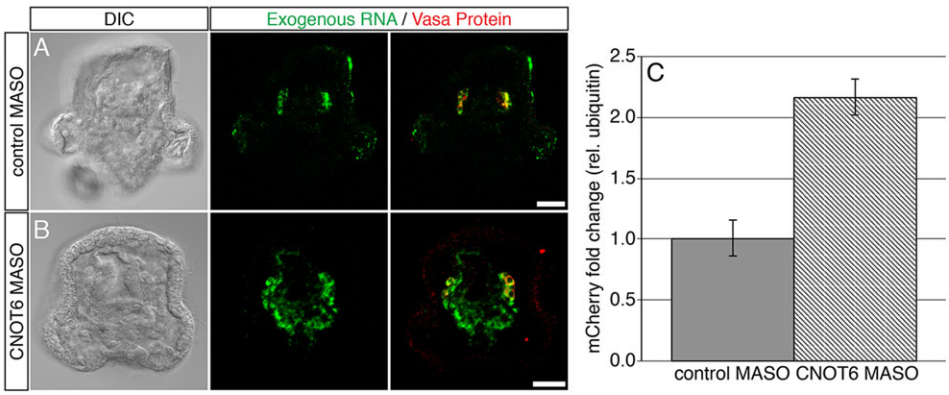

Fig. 7. CNOT6 regulates general retention of exogenous RNA in the sMics. (A,B) FISH for injected RNA containing the mCherry open reading frame and SV40 3′ polyadenylation signal. This transcript is normally retained only in sMics at 96 hpf (A), but is retained broadly throughout the endomesoderm with CNOT6 knockdown (B). (C) qPCR for exogenous mCherry RNA at 96 hpf. With CNOT6 knockdown, mCherry levels increase twofold. Scale bars: 20 µm.

Development (2014) 141, 3134-3142 doi:10.1242/dev.110395

Illumina technology (described below). Helicos run statistics are listed in supplementary material Table S3.

Illumina sample preparation, deep sequencing and reference transcriptome assembly

RNA was extracted from several developmental stages, including ovary, 32-cell stage, 15 h blastula, 41 h gastrula and 4-day pluteus, using the RNEasy Mini kit (Qiagen) with on-column DNAse. The isolated RNA was processed through standard procedures using the Illumina mRNA-Seq kit and sequenced on a single lane of a GAIIx using a read length of 105 bp with paired ends. The transcriptome was assembled using Velvet (1.0.09) and Oases (0.1.14) with a k-mer of 31 (Schulz et al., 2012). Exemplar sequences were selected from each locus based on abundance with a minimum length cutoff. The exemplar sequences were annotated with Blast2GO and compared by BLAST (minimum score of $1E^{-5}$) with the *S. purpuratus* SPU gene predictions (Conesa et al., 2005; Sodergren et al., 2006). All Helicos reads, *de novo* transcriptome reads and the assembled transcriptome are available under BioProject PRJNA188114.

Whole-mount *in situ* hybridization (WMISH) and immunofluorescence

WMISH was performed as described previously (Juliano et al., 2006). Nanos probe generation is described by Juliano et al. (2010). Approximately 1 kb antisense probe templates were PCR-amplified from cDNA using a reverse primer tailed with the T7 promoter. Digoxygenin-labeled antisense probes were transcribed using the Roche DIG RNA labeling kit according to the manufacturer's instructions. Embryos of mixed developmental stages were fixed with MOPS-buffered PFA and hybridized for at least 5 days at 50°C with 70% formamide and 0.5 ng/µl probe. Hybridization was then visualized using either NBT/BCIP chromogenic detection or tyramide fluorescence amplification (TSA plus system, PerkinElmer). Vasa immunofluorescence was performed as described previously (Voronina et al., 2008). Rabbit antibodies to RNAP pSer2 and H3K9me3 were obtained from Abcam (ab5095 and ab8898, respectively; both 1:500). As the Vasa antibody was also raised in rabbit, co-labeling (e.g. Fig. 2) was performed as follows. Embryos were incubated with Vasa antibody (1:250) overnight at room temperature in PBST (0.1% Triton X-100, pH 7.4). The embryos were washed four times and then incubated 3 h at room temperature with rhodamine-labeled goat anti-rabbit Fab fragments. This procedure was then repeated sequentially with the pSer2 or H3K9me3 antibodies with FITC-labeled Fab fragments. Primer sequences used to amplify probe templates are listed in supplementary material Table S4. EdU lineage tracing of the sMics was performed with the Click-IT EdU imaging kit (Life Technologies). Briefly, embryos were soaked in 10 µM EdU in FSW from fertilization until first cleavage, washed six times with FSW and allowed to develop until the desired stage. *In situ* hybridization (ISH) was then performed as described above. Following hybridization, EdU was detected with fluorescent azide according to the manufacturer's instructions. Finally, the *in situ* probes were detected as described above.

Cloning and reporter constructions

DNA fragments were PCR-amplified and cloned by standard methods. For overexpression studies, constructs were built in a modified pCS2 vector containing additional rare 8-base cutting restriction enzyme sites (Gökirmak et al., 2012). PRE mutant reporter constructs were generated by site-directed mutagenesis with the QuikChange II kit (Agilent Technologies). Primers used for generating these constructs are listed in supplementary material Table S5.

MASO and mRNA microinjection

Custom MASOs were synthesized by GeneTools. The control MASO targets a divergent Nanos ortholog in a distantly related sea star species (*Patiria miniata*). MASO injection solutions contained 20% glycerol and 100 µg/ml 10,000 MW Texas Red-Lysine or FITC dextran. MASOs were used at working concentrations listed below. Synthetic mRNAs were transcribed using the mMessage mMachine SP6 or T7 kit (Ambion) from linearized plasmid template. Eggs were dejellied by incubating for 10 min in pH 5.0 seawater and arranged in rows on protamine sulfate-coated Petri dishes. Fertilized eggs were injected with approximately 2 pl of MASO or RNA by constant pressure injection in the presence of 1 mM 3-AT (Sigma). The injected zygotes were then washed in filtered seawater and incubated at 15°C. Custom morpholino sequences are listed in supplementary material Table S6.

RNA isolation and qPCR

RNA for qPCR was isolated with the RNEasy Micro kit with on column DNAse (Qiagen). First-strand cDNA synthesis was performed using MultiScribe reverse transcriptase (Invitrogen). qPCR was performed using an ABI 7900 real-time instrument with Fast Start Universal SYBR master mix (Roche). Four embryo equivalents of cDNA were used per reaction, which yielded CT values in the 20-30 range. Experiments were run in triplicate and normalized to ubiquitin. To account for variability in the amount of injected mCherry RNA, the 96 h time points were normalized to the mCherry levels tested at 18 hpf, a time point before RNA retention becomes apparent and therefore representative of the amount of RNA injected. mCherry qPCR primer sequences were as follows: F, 5′-CCCCGTAATGCAGAAGAAGA-3′; R, 5′-TCTTGGCCTTGTAGGTGGTC-3′.

Acknowledgements

We thank Stefanie Terrizzi and Emma Riley for assistance with FACS; Casey Dunn, Mark Howison and Jason Wood for computational expertise and helpful discussions; Geoff Williams for imaging assistance; Celina Juliano for critical feedback; TGZ for tuff feedback and Novartis for providing PSC-833. Transcriptome analysis was conducted using computational resources and services at the Center for Computation and Visualization, Brown University, USA.

Competing interests

The authors declare no competing financial interests.

Author contributions

G.M.W. and S.Z.S. conceived the project; S.Z.S., J.P.C. and A.H. developed FACS methods; S.Z.S. and N.O. performed experiments. A.M.R. performed bioinformatics analyses; T.R. and P.M.M. performed Helicos sequencing; and S.Z.S. and G.M.W. wrote the manuscript, which was edited by A.M.R., N.O., J.P.C. and A.H.

Funding

This work was supported by the National Institutes of Health [F31 AG041637 to S.Z.S.; 2R01HD028152 to G.M.W.] and the National Science Foundation [IOS-1120972 to G.M.W.]. Deposited in PMC for release after 12 months.

Supplementary material

Supplementary material available online at
http://dev.biologists.org/lookup/suppl/doi:10.1242/dev.110395/-/DC1

References

Bashirullah, A., Halsell, S. R., Cooperstock, R. L., Kloc, M., Karaiskakis, A., Fisher, W. W., Fu, W., Hamilton, J. K., Etkin, L. D. and Lipshitz, H. D. (1999). Joint action of two RNA degradation pathways controls the timing of maternal transcript elimination at the midblastula transition in Drosophila melanogaster. *EMBO J.* **18**, 2610-2620.

Bushati, N., Stark, A., Brennecke, J. and Cohen, S. M. (2008). Temporal reciprocity of miRNAs and their targets during the maternal-to-zygotic transition in Drosophila. *Curr. Biol.* **18**, 501-506.

Buss, L. W. (1987). *The Evolution of Individuality*. Princeton: Princeton University Press.

Campanale, J. P. and Hamdoun, A. (2012). Programmed reduction of ABC transporter activity in sea urchin germline progenitors. *Development* **139**, 783-792.

Chen, D., Zheng, W., Lin, A., Uyhazi, K., Zhao, H. and Lin, H. (2012). Pumilio 1 suppresses multiple activators of p53 to safeguard spermatogenesis. *Curr. Biol.* **22**, 420-425.

Collart, M. A. and Panasenko, O. O. (2012). The Ccr4-Not complex. *Gene* **492**, 42-53.

Conesa, A., Götz, S., García-Gómez, J. M., Terol, J., Talón, M. and Robles, M. (2005). Blast2GO: a universal tool for annotation, visualization and analysis in functional genomics research. *Bioinformatics* **21**, 3674-3676.

Ewen-Campen, B., Schwager, E. E. and Extavour, C. G. M. (2010). The molecular machinery of germ line specification. *Mol. Reprod. Dev.* **77**, 3-18.

Extavour, C. G. M. (2007). Evolution of the bilaterian germ line: lineage origin and modulation of specification mechanisms. *Integr. Comp. Biol.* **47**, 770-785.

Extavour, C. G. and Akam, M. (2003). Mechanisms of germ cell specification across the metazoans: epigenesis and preformation. *Development* **130**, 5869-5884.

Gerber, A. P., Luschnig, S., Krasnow, M. A., Brown, P. O. and Herschlag, D. (2006). Genome-wide identification of mRNAs associated with the translational regulator PUMILIO in Drosophila melanogaster. *Proc. Natl. Acad. Sci. USA* **103**, 4487-4492.

Giraldez, A. J., Mishima, Y., Rihel, J., Grocock, R. J., Van Dongen, S., Inoue, K., Enright, A. J. and Schier, A. F. (2006). Zebrafish MiR-430 promotes deadenylation and clearance of maternal mRNAs. *Science* **312**, 75-79.

Gökirmak, T., Campanale, J. P., Shipp, L. E., Moy, G. W., Tao, H. and Hamdoun, A. (2012). Localization and substrate selectivity of sea urchin multidrug (MDR) efflux transporters. *J. Biol. Chem.* **287**, 43876-43883.

Gustafson, E. A. and Wessel, G. M. (2010). Exogenous RNA is selectively retained in the small micromeres during sea urchin embryogenesis. *Mol. Reprod. Dev.* **77**, 836.

Gustafson, E. A., Yajima, M., Juliano, C. E. and Wessel, G. M. (2011). Post-translational regulation by gustavus contributes to selective Vasa protein accumulation in multipotent cells during embryogenesis. *Dev. Biol.* **349**, 440-450.

Juliano, C. E., Voronina, E., Stack, C., Aldrich, M., Cameron, A. R. and Wessel, G. M. (2006). Germ line determinants are not localized early in sea urchin development, but do accumulate in the small micromere lineage. *Dev. Biol.* **300**, 406-415.

Juliano, C. E., Yajima, M. and Wessel, G. M. (2010). Nanos functions to maintain the fate of the small micromere lineage in the sea urchin embryo. *Dev. Biol.* **337**, 220-232.

Kedde, M., Strasser, M. J., Boldajipour, B., Oude Vrielink, J. A. F., Slanchev, K., le Sage, C., Nagel, R., Voorhoeve, P. M., van Duijse, J., Ørom, U. A. et al. (2007). RNA-binding protein Dnd1 inhibits microRNA access to target mRNA. *Cell* **131**, 1273-1286.

Le Borgne, R. and Schweisguth, F. (2003). Notch signaling: endocytosis makes delta signal better. *Curr. Biol.* **13**, R273-R275.

Lessard, J. A. and Crabtree, G. R. (2010). Chromatin regulatory mechanisms in pluripotency. *Annu. Rev. Cell Dev. Biol.* **26**, 503-532.

Lipson, D., Raz, T., Kieu, A., Jones, D. R., Giladi, E., Thayer, E., Thompson, J. F., Letovsky, S., Milos, P. and Causey, M. (2009). Quantification of the yeast transcriptome by single-molecule sequencing. *Nat. Biotechnol.* **27**, 652-658.

Miller, J. R. and McClay, D. R. (1997). Characterization of the role of cadherin in regulating cell adhesion during sea urchin development. *Dev. Biol.* **192**, 323-339.

Mishima, Y., Giraldez, A. J., Takeda, Y., Fujiwara, T., Sakamoto, H., Schier, A. F. and Inoue, K. (2006). Differential regulation of germline mRNAs in soma and germ cells by zebrafish miR-430. *Curr. Biol.* **16**, 2135-2142.

Nakamura, A. and Seydoux, G. (2008). Less is more: specification of the germline by transcriptional repression. *Development* **135**, 3817-3827.

Oliveri, P., Carrick, D. M. and Davidson, E. H. (2002). A regulatory gene network that directs micromere specification in the sea urchin embryo. *Dev. Biol.* **246**, 209-228.

Oulhen, N. and Wessel, G. M. (2013). Retention of exogenous mRNAs selectively in the germ cells of the sea urchin requires only a 5′-cap and a 3′-UTR. *Mol. Reprod. Dev.* **80**, 561-569.

Pehrson, J. R. and Cohen, L. H. (1986). The fate of the small micromeres in sea urchin development. *Dev. Biol.* **113**, 522-526.

Rouget, C., Papin, C., Boureux, A., Meunier, A.-C., Franco, B., Robine, N., Lai, E. C., Pelisson, A. and Simonelig, M. (2010). Maternal mRNA deadenylation and decay by the piRNA pathway in the early Drosophila embryo. *Nature* **467**, 1128-1132.

Schulz, M. H., Zerbino, D. R., Vingron, M. and Birney, E. (2012). Oases: robust de novo RNA-seq assembly across the dynamic range of expression levels. *Bioinformatics* **28**, 1086-1092.

Semotok, J. L., Cooperstock, R. L., Pinder, B. D., Vari, H. K., Lipshitz, H. D. and Smibert, C. A. (2005). Smaug recruits the CCR4/POP2/NOT deadenylase complex to trigger maternal transcript localization in the early Drosophila embryo. *Curr. Biol.* **15**, 284-294.

Seydoux, G. and Braun, R. E. (2006). Pathway to totipotency: lessons from germ cells. *Cell* **127**, 891-904.

Seydoux, G. and Dunn, M. A. (1997). Transcriptionally repressed germ cells lack a subpopulation of phosphorylated RNA polymerase II in early embryos of Caenorhabditis elegans and Drosophila melanogaster. *Development* **124**, 2191-2201.

Shirae-Kurabayashi, M., Matsuda, K. and Nakamura, A. (2011). Ci-Pem-1 localizes to the nucleus and represses somatic gene transcription in the germline of Ciona intestinalis embryos. *Development* **138**, 2871-2881.

Sodergren, E., Weinstock, G. M., Davidson, E. H., Cameron, R. A., Gibbs, R. A., Angerer, R. C., Angerer, L. M., Arnone, M. I., Burgess, D. R., Burke, R. D. et al.; **Sea Urchin Genome Sequencing Consortium** (2006). The Genome of the Sea Urchin Strongylocentrotus purpuratus. *Science* **314**, 941-952.

Song, J. L., Stoeckius, M., Maaskola, J., Friedländer, M., Stepicheva, N., Juliano, C., Lebedeva, S., Thompson, W., Rajewsky, N. and Wessel, G. M. (2012). Select microRNAs are essential for early development in the sea urchin. *Dev. Biol.* **362**, 104-113.

Suzuki, A., Saba, R., Miyoshi, K., Morita, Y. and Saga, Y. (2012). Interaction between NANOS2 and the CCR4-NOT deadenylation complex is essential for male germ cell development in mouse. *PLoS ONE* **7**, e33558.

Takeda, Y., Mishima, Y., Fujiwara, T., Sakamoto, H. and Inoue, K. (2009). DAZL relieves miRNA-mediated repression of germline mRNAs by controlling poly(A) tail length in zebrafish. *PLoS ONE* **4**, e7513.

Tanaka, S. and Dan, K. (1990). Study of the lineage and cell cycle of small micromeres in embryos of the sea urchin, hemicentrotus pulcherrimus. (small micromeres/cell cycle/cell lineage/unequal cleavage/sea urchin). *Dev. Growth Differ.* **32**, 145-156.

Van Etten, J., Schagat, T. L., Hrit, J., Weidmann, C. A., Brumbaugh, J., Coon, J. J. and Goldstrohm, A. C. (2012). Human Pumilio proteins recruit multiple deadenylases to efficiently repress messenger RNAs. *J. Biol. Chem.* **287**, 36370-36383.

Voronina, E., Lopez, M., Juliano, C. E., Gustafson, E., Song, J. L., Extavour, C., George, S., Oliveri, P., McClay, D. and Wessel, G. (2008). Vasa protein expression is restricted to the small micromeres of the sea urchin, but is inducible in other lineages early in development. *Dev. Biol.* **314**, 276-286.

Wei, Z., Angerer, R. C. and Angerer, L. M. (2006). A database of mRNA expression patterns for the sea urchin embryo. *Dev. Biol.* **300**, 476-484.

Weidmann, C. A. and Goldstrohm, A. C. (2012). Drosophila Pumilio protein contains multiple autonomous repression domains that regulate mRNAs independently of Nanos and brain tumor. *Mol. Cell. Biol.* **32**, 527-540.

White, E. K., Moore-Jarrett, T. and Ruley, H. E. (2001). PUM2, a novel murine puf protein, and its consensus RNA-binding site. *RNA* **7**, 1855-1866.

Wreden, C., Verrotti, A. C., Schisa, J. A., Lieberfarb, M. E. and Strickland, S. (1997). Nanos and pumilio establish embryonic polarity in Drosophila by promoting posterior deadenylation of hunchback mRNA. *Development* **124**, 3015-3023.

Yajima, M. and Wessel, G. M. (2011). Small micromeres contribute to the germline in the sea urchin. *Development* **138**, 237-243.

Yajima, M. and Wessel, G. M. (2012). Autonomy in specification of primordial germ cells and their passive translocation in the sea urchin. *Development* **139**, 3786-3794.

Yajima, M., Gustafson, E. A., Song, J. L. and Wessel, G. M. (2013). Piwi regulates Vasa accumulation during embryogenesis in the sea urchin. *Dev. Dyn.* **243**, 451-458.

Zaessinger, S., Busseau, I. and Simonelig, M. (2006). Oskar allows nanos mRNA translation in Drosophila embryos by preventing its deadenylation by Smaug/CCR4. *Development* **133**, 4573-4583.

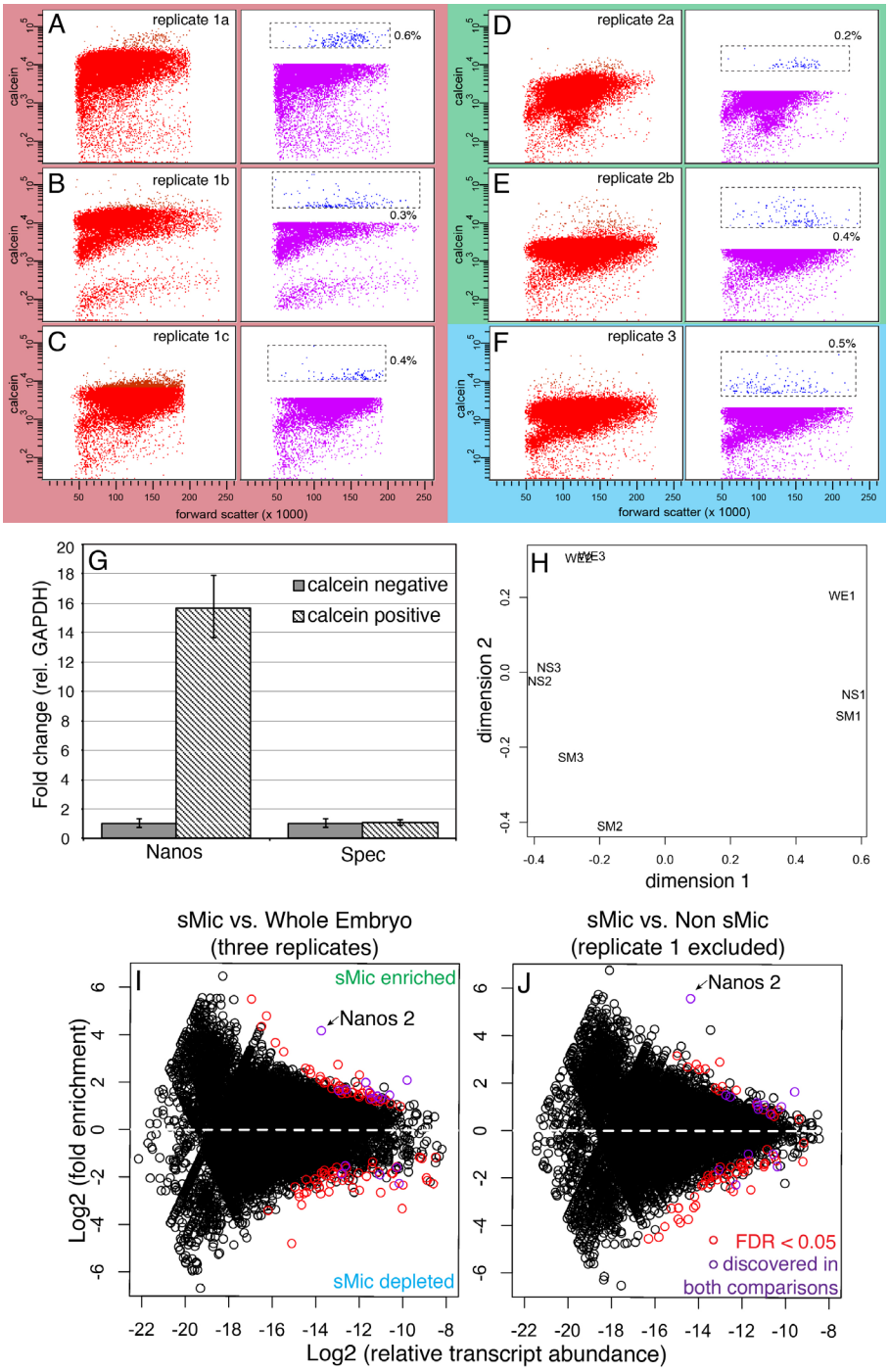

Figure S1, related to Figures 1. FACS isolation of sMics and transcriptomic analysis. (A-F) Scatter plot representations of FACS sorts for three biological replicates. Replicate 1 (A-C, red background) consisted of three sorts of embryos derived from distinct parental crosses. Replicate 2 (D-E, green background) consisted of two sorts from two parental crosses. Replicate 3 (F, blue background) was sorted from a single parental cross. Red points indicate the total cell population, blue points indicate the collected calcein+ cells, and purple points indicate collected calcein— cells. Percentages represent fraction of collected calcein+ cells relative to the whole population. (G) qPCR for Nanos indicates enrichment of sMics in the calcein+ fraction, as opposed for Spec, an ectodermal negative control. (H) Multidimensional scaling (MDS) analysis of replicate transcriptomes for isolated sMics (SM1-3), non-sMics (NS1-3), and whole embryo (WE1-3). Replicate 2 and 3 samples were highly related with whole embryo, sMic, and non-sMic transcriptomes clustering separately. Replicate 1 samples are outliers, showing low relatedness to the others in both dimensions, and poor separation between SM and NS samples. This variation likely points to issues with sample handling (RNA collection, or RNA-seq sample preparation) or less efficient calcein labeling. In subsequent differential expression analysis, we therefore made comparisons both with and without including Replicate 1 samples. (I,J) Smear plot depiction of differentially expressed genes. (I) sMic vs. Whole Embryo with replicate 1 included, and (J) sMic vs. non-sMic with replicate 1 excuded are considered here. Transcripts are represented by open circles, with fold enrichment in the sMics on the y-axis and relative transcript abundance on the x-axis. Transcripts meeting a significance threshold of 0.05 (false discovery rate, FDR) are in red; transcripts identified in both comparisons are in purple. Arrows indicate the previously identified sMic factor Nanos2.

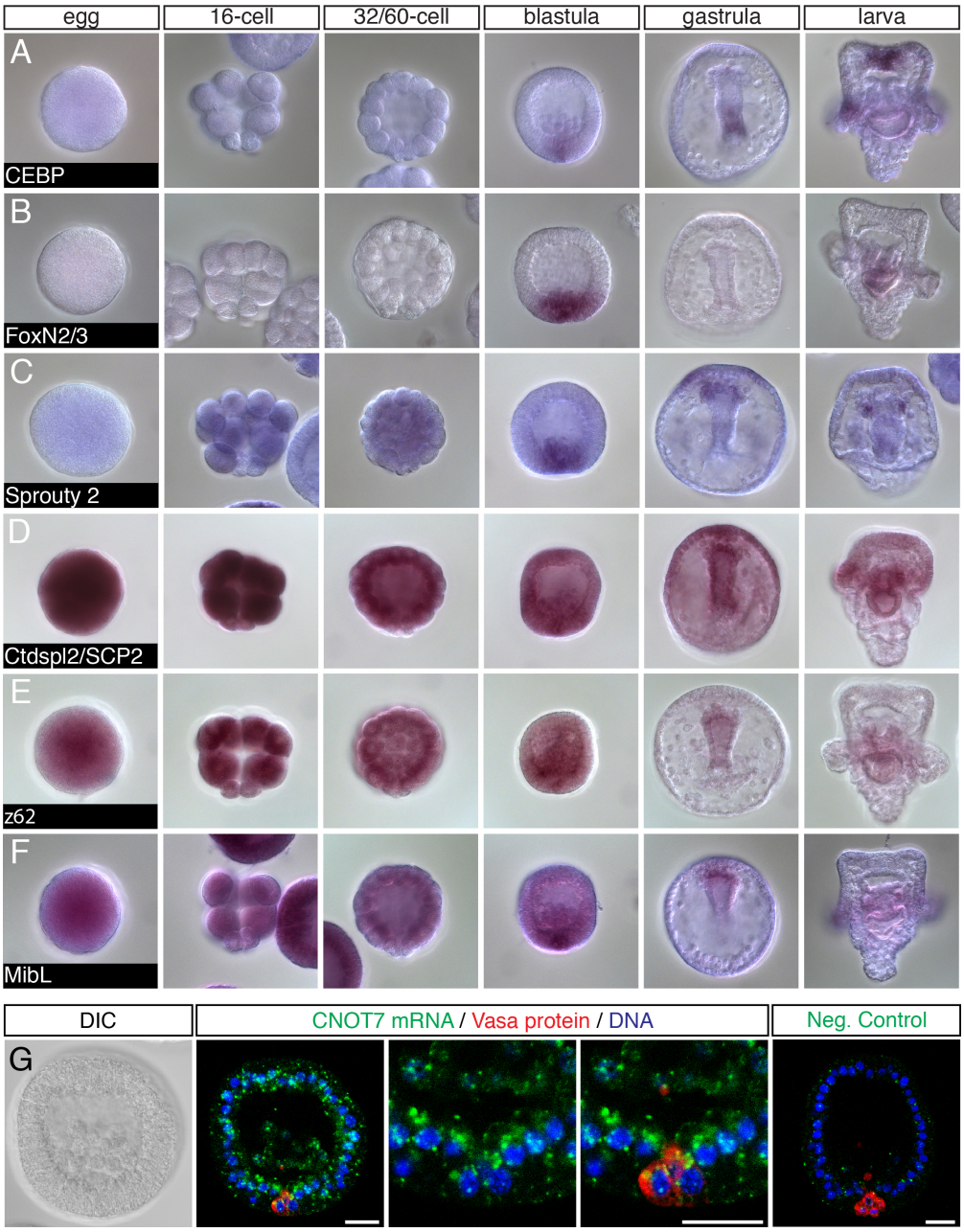

Figure S2, related to Figures 1 and 3. WMISH for selected transcripts. (A-F) WMISH for sMic-enriched transcripts identified through differential expression analysis. (G) The S. purpuratus genome contains two CNOT-related nucleases: CNOT6 and CNOT7. Unlike CNOT6, which is specifically depleted in the sMics, CNOT7 transcript (green) is ubiquitously distributed. sMics are labeled in red with vasa antibody.

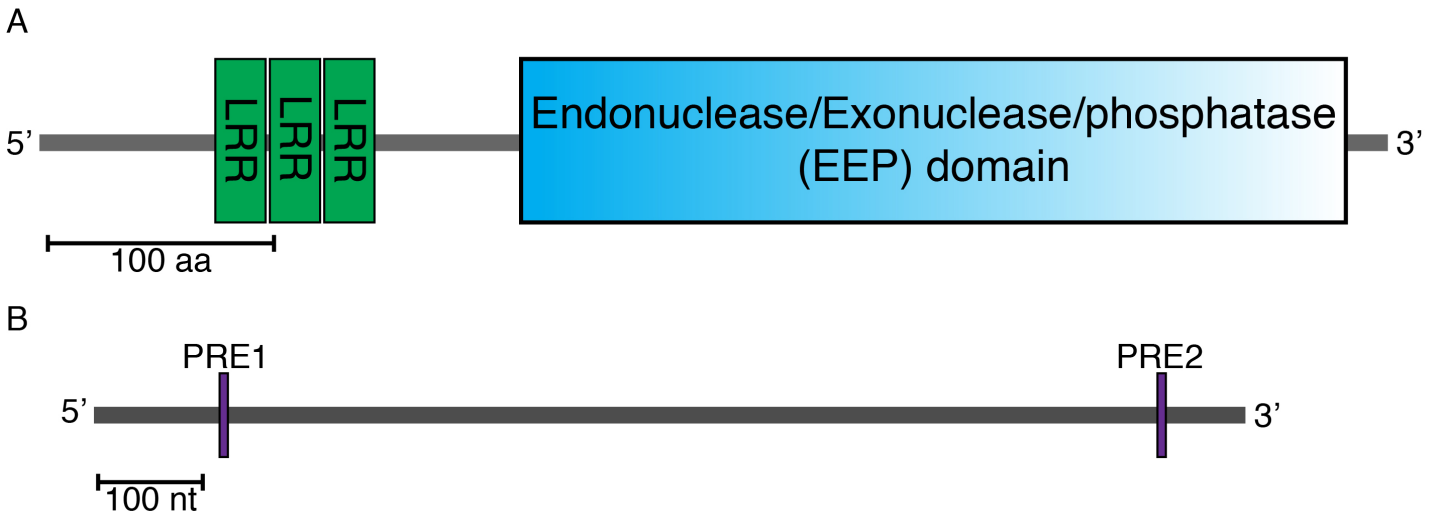

Figure S3, related to Figure 4. Organization of the CNOT6 open reading frame and 3'UTR. (A) Domain organization of CNOT6 predicted by PFAM (Punta et al., 2012). (B) Schematic of PRE motifs within the CNOT6 3'UTR and full-length sequence.

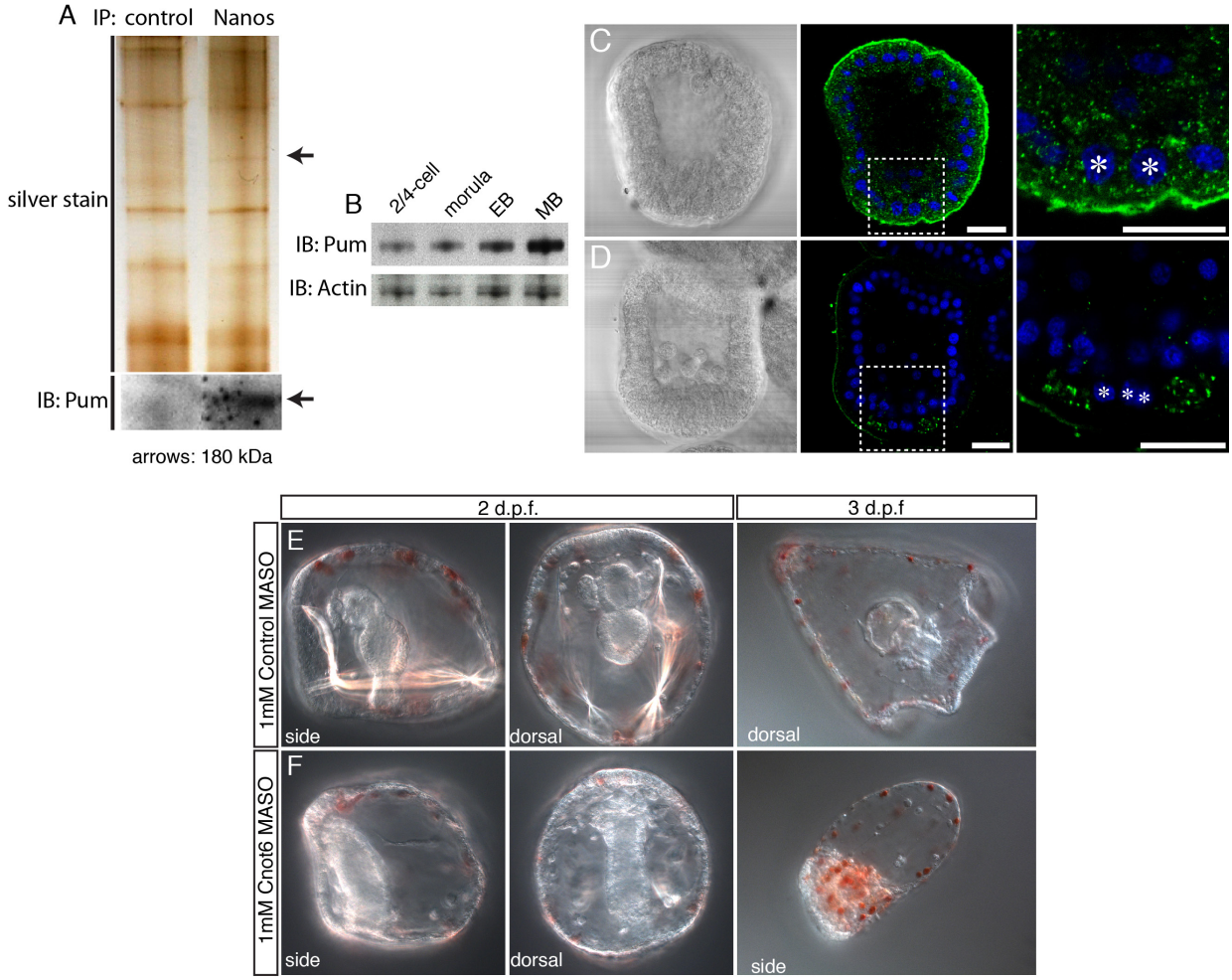

Figure S4, related to Figure 3 and 4. (A) Association of Nanos and Pumilio. Compared to Vasa antibody control, Nanos antibody specifically pulls down a 180 kDa band recognized by silver stain and Pumilio immunoblot. (B) Temporal expression of Pumilio. Pumilio is detectable in early embryos, and increases in abundance through early blastulae (EB) and mesenchyme blastulae (MB) stages. (C,D) Spatial localization of Pumilio protein. Pumilio is detectable in granule structures in all cells, including the sMics, of early blastula (C), but becomes highly enriched in the Veg2 mesodermal precursors after primary mesenchyme ingression (D). Asterisks indicate sMic nuclei. (E,F) Injection of 1mM CNOT6 MASO 1 results in failure to produce skeletons or a tripartite gut. By 3 days, the endoderm degenerates into mesenchyme-like cells.

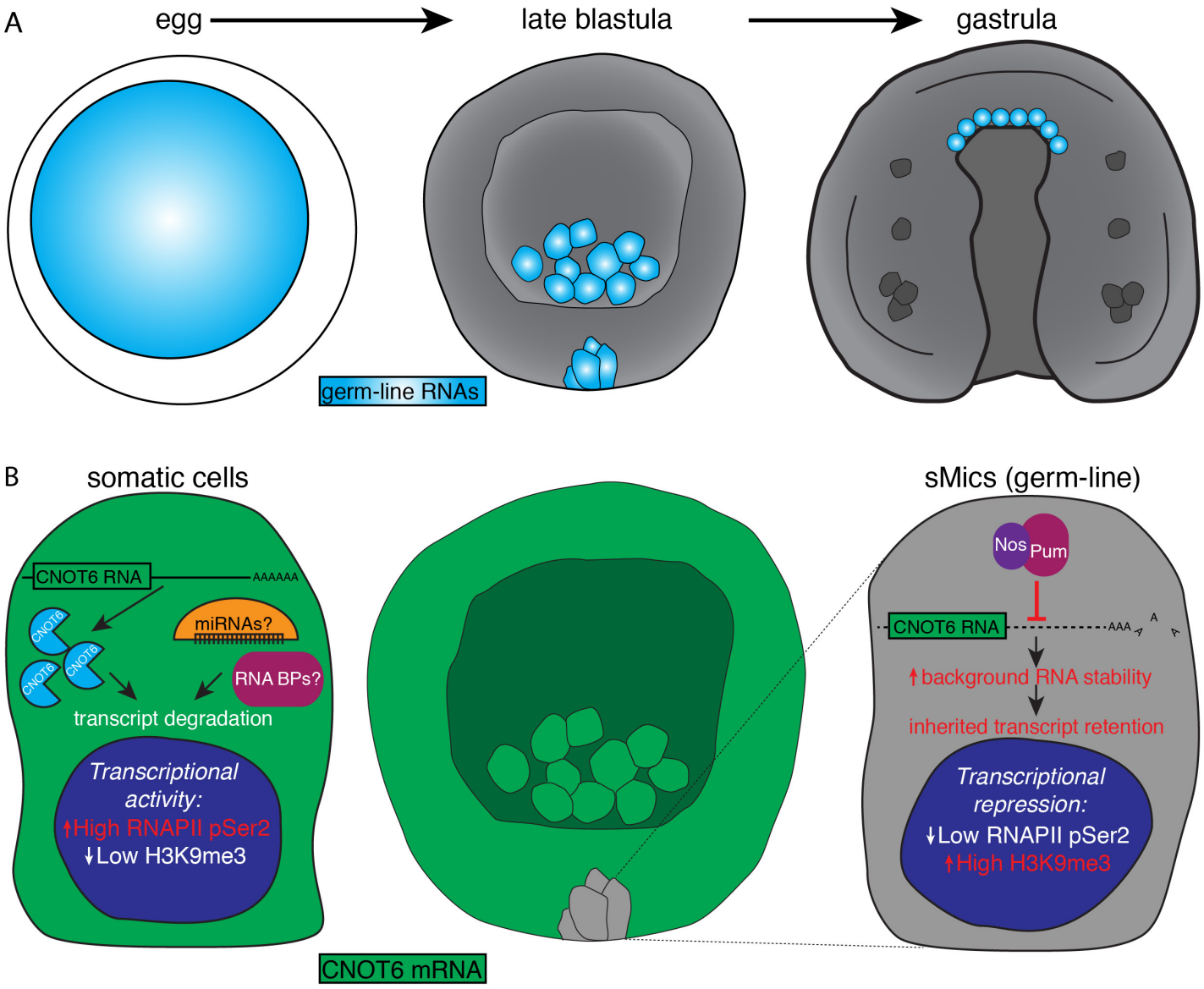

Figure S5. Model. Time capsule model for germ line development. (A) Maternally deposited mRNAs are coordinately degraded in somatic cells at blastula/gastrula stage but stabilized in the sMics. (B) Mechanism for sMic segregation. CNOT6 transcript is in green, and is present in all cells except sMics (gray), where Nanos/Pumilio (Nos/Pum) represses it. This repression creates a stable environment for inherited RNA. Conversely, CNOT6 protein accumulates in somatic cells, where it may act in parallel with and/or downstream of miRNA and RNA binding protein (BP) mediated degradation.

Supplementary References

Punta, M., Coggill, P. C., Eberhardt, R. Y., Mistry, J., Tate, J., Boursnell, C., Pang, N., Forslund, K., Ceric, G., Clements, J., et al. (2012). The Pfam protein families database. *Nucleic Acids Res* **40**, D290–301.

Table S1, related to Figure 1. Gene set enrichment analysis of the union sets of 78 sMic enriched transcripts, and 152 sMic-depleted transcripts. Analysis was performed using the topGO Bioconductor package. *P*-values are by Fisher's exact test.

sMic-enriched categories			sMic-depleted categories		
GO ID	**Term**	**p-val**	**GO ID**	**Term**	**p-val**
0003676	nucleic acid binding	4.40E-05	0005198	structural molecule activity	4.50E-08
0000988	protein binding transcription factor act...	0.0015	0032561	guanyl ribonucleotide binding	0.0042
0000989	transcription factor binding transcripti...	0.0015	0019001	guanyl nucleotide binding	0.0045
0003712	transcription cofactor activity	0.0015	0005201	extracellular matrix structural constitu...	0.0053
0043565	sequence-specific DNA binding	0.0049	0015399	primary active transmembrane transporter...	0.01
0008134	transcription factor binding	0.006	0015405	P-P-bond-hydrolysis-driven transmembrane...	0.01
0008349	MAP kinase kinase kinase kinase activity	0.0067	0004683	calmodulin-dependent protein kinase acti...	0.016
0043425	bHLH transcription factor binding	0.0067	0004197	cysteine-type endopeptidase activity	0.0212
0043426	MRF binding	0.0067	0022804	active transmembrane transporter activit...	0.0228
0005488	binding	0.0086	0004674	protein serine/threonine kinase activity	0.0237
0035258	steroid hormone receptor binding	0.0178	0003723	RNA binding	0.0287
0003729	mRNA binding	0.0189	0016289	CoA hydrolase activity	0.0368
0035257	nuclear hormone receptor binding	0.0224	0050839	cell adhesion molecule binding	0.0368
0051427	hormone receptor binding	0.0275			
0090079	translation regulator activity, nucleic ...	0.0328			
0003677	DNA binding	0.0389			
0042974	retinoic acid receptor binding	0.0393			
0045182	translation regulator activity	0.0393			
0008092	cytoskeletal protein binding	0.0433			
0032561	guanyl ribonucleotide binding	0.0446			
0046332	SMAD binding	0.0457			
0019001	guanyl nucleotide binding	0.0467			

Table S2. Summary of FACS replicates and RNA extraction yields.

	sMic	non-sMic	whole embryo
Replicate 1 *(3 pooled parental crosses)*	700 ng RNA 113,191 cells	1800 ng RNA 618,511 cells	3800 ng RNA
Replicate 2 *(2 pooled parental crosses)*	1080 ng RNA 213,174 cells	1820 ng RNA 892,329 cells	6700 ng RNA
Replicate 3 *(1 parental cross)*	350 ng RNA 55,571 cells	1278 ng RNA 438,938 cells	1508 ng RNA

Table S3. Helicos run statistics.

Sample Name	Total Filtered Reads	Mean Read Length (nt)	Percent aligned reads	Sequencing Error Rate
WE1	27,035,746	31.21	49.08%	6.95%
SMM1	25,331,121	31.15	44.29%	6.86%
NSM1	30,889,594	31.27	42.25%	7.02%
WE2	14,670,195	33.75	60.12%	5.44%
SMM2	15,096,355	33.28	60.84%	5.49%
NSM2	12,043,418	34.24	57.30%	5.63%
WE3	14,450,706	33.84	54.68%	5.89%
SMM3	8,300,956	33.66	56.06%	5.62%
NSM3	10,630,234	34.15	58.47%	5.69%

Table S4. Primers used for generation of template DNA for ISH probe transcription.

Primer Name	Sequence
Baf250	**F:** TCGACAACCACCACTACCAA **R:** taatacgactcactatagggTGTTGTTCACTCCACCCGTA
CEBP	**F:** AGGGCTGAGGTACAGCAGAA **R:** taatacgactcactatagggCCCTCGACACGTTTCTTTA
FoxN2/3	**F:** CGAATGGACAAAGGACCACT **R:** taatacgactcactatagggCTTGGTGATGGGGTACACT
Sprouty2	**F:** GCTCTGTTCCCTTGAGCAAC **R:** taatacgactcactatagggGCAGGGATCATCCGTACAGT
Ctdspl2/SCP2	**F:** AAGCCACCAATCCTGTGTTC **R:** taatacgactcactatagggCAGAAAGGCACAAGCAATCA
z62	**F:** AGTCTAGCAAATGGCGTCGT **R:** taatacgactcactatagggATGTAACCACATTCGCAGCA
MibL	**F:** CTGGACAGACACCAGAGCAA **R:** taatacgactcactatagggCATCTGCTCCGTGCATAAGA
CNOT6	**F:** GCAGGTGCTAGGTCTGAAGG **R:** taatacgactcactatagggCGAGTTGGAGGAGAAGTTGC
CNOT7	**F:** TGCCAACTCAAACCAATGAA **R:** taatacgactcactatagggGCACCCTGGTTAAAAGGTCA

Table S5. Primers used for CNOT6 reporter constructions.

Primer Name (description)	Sequence
CNOT6 3'UTR (reporter construct)	**F:** GGGACTCAGGGTGGTGTTC **R:** ACAGAGAATTGCACATTGGTTGG
PRE1 (site-directed mutagenesis)	**F:** TTCGTACTTTGTACAGTGaaaAAATTGATGCTATTTTGC **R:** GCAAAATAGCATCAATTTtttCACTGTACAAAGTACGAA
PRE2 (site-directed mutagenesis)	**F:** ATTTGAGACCATGGGTTGaaaAAATGAGGATTTGAACCA **R:** TGGTTCAAATCCTCATTTtttCAACCCATGGTCTCAAAT

Table S6. Custom morpholino sequences used.

MASO Name	Sequence	Concentration of injection solution
Nanos	GTGACTAAAGTGCGTGGAAACTCGA	500 µM
Pumilio	TTTCCTTCTATGATACAGACCCGCT	100 µM
CNOT6 1	ATTTATCTTTGGGCATCCTGGTGGC	500 µM
CNOT6 2	GTCGGTTTTCACCAGTTCAGGAGGC	500 µM
PRE1	AATAGCATCAATTTACACACTGTAC	1000 µM
PRE2	GTTCAAATCCTCATTTACACAACCC	1000 µM

Table S7.

Download Table S7

Table S8.

Download Table S8

Table S9.

Download Table S9